

**Interstellar Absorption Lines in the spectrum of the starburst
galaxy NGC 1705¹**

M. S. Sahu

NASA/Goddard Space Flight Center, Code 681, Greenbelt, MD 20771

and

National Optical Astronomy Observatories, 950 N. Cherry Avenue, Tucson, AZ 8519-4933

msahu@panke.gsfc.nasa.gov

Received 22 May 1998; accepted 1 June 1998

To appear in AJ, September 1998 issue

¹Based on observations taken with the NASA/ESA *Hubble Space Telescope*, obtained at the Space Telescope Science Institute, which is operated by the Association of the Universities for Research in Astronomy under contract NAS 5-26555

ABSTRACT

I present a *GHERS* archival study of the interstellar absorption lines in the line-of-sight to the H I-rich starburst dwarf galaxy NGC 1705, in the $\lambda 1170$ to 1740 \AA range at $\sim 120 \text{ km s}^{-1}$ resolution. The absorption features arising due to photospheric lines are distinctly different from the interstellar lines : the photospheric lines are weak, broad (equivalent widths $> 1 \text{ \AA}$), asymmetric and centred around the systemic LSR velocity of NGC 1705 ($\sim 610 \text{ km s}^{-1}$). The interstellar lines consist of three relatively narrow components at LSR velocities of -20 , 260 and 540 km s^{-1} and include absorption by neutral atoms (N I $\lambda 1200 \text{ \AA}$ triplet and O I $\lambda 1302 \text{ \AA}$) singly ionized atoms (Si II $\lambda 1190$, 1193 , 1260 , 1304 and 1526 \AA , S II $\lambda 1253 \text{ \AA}$, C II $\lambda 1334 \text{ \AA}$, C II* $\lambda 1336 \text{ \AA}$, Fe II $\lambda 1608 \text{ \AA}$ and Al II $\lambda 1670 \text{ \AA}$) and atoms in higher ionization states (Si III $\lambda 1206 \text{ \AA}$, Si IV $\lambda 1393$, 1402 \AA and C IV $\lambda 1548$, 1550 \AA). The Si IV and C IV absorption features have both interstellar and photospheric contributions.

In an earlier study, Sahu & Blades (1997) identified the absorption system at -20 km s^{-1} with Milky Way disk/halo gas and the 260 km s^{-1} system with a small, isolated high-velocity cloud HVC 487, which is probably associated with Magellanic Stream gas. The 540 km s^{-1} absorption system is associated with a kpc-scale expanding, ionized supershell centred on the superstar cluster NGC 1705-1. The analysis presented in this paper consists of (1) a list of all interstellar absorption features with $> 3 \sigma$ significance and their measured equivalent widths and (2) plots of the lines in the various atomic species together with the results of non-linear least square fit profiles to the observed data and (3) unpublished 21-cm maps from the Wakker & van Woerden survey showing the large-scale H I distribution in the region near the NGC 1705 sightline and HVC 487. Further, I report weak N I $\lambda 1200 \text{ \AA}$ triplet absorption for the supershell component, which in the absence of dust depletion and

ionization corrections implies a low N abundance. A low N abundance for the supershell is consistent with an interpretation of nucleosynthetic enrichment by time-delayed *primary* nitrogen production, the age estimate of $10 - 20 \times 10^6$ years for the central superstar cluster NGC 1705-1 (Heckman and Leitherer, 1997) and the underabundance of Fe reported by Sahu and Blades. However, using the N I 1200Å triplet alone to estimate the total N abundance could result in a severe underestimation of this quantity: although N does not deplete onto interstellar dust grains, photoionization and collisional ionization effects could increase the fraction of N found in higher ionization stages. Uncertainties in the total N abundance caused by photoionization and collisional ionization effects can only be addressed by future observations of the higher ionization lines, namely, N II λ 1084 Å and N III λ 989 Å.

Subject headings: galaxies: ISM — ultraviolet: spectra — galaxies: individual
(NGC 1705)

1. Introduction

Absorption features in the line-of-sight to nearby galaxies provide a tool to study the properties of gas associated with three different environments, namely, gas in our Galaxy, gas associated with the background target galaxy and gas in the sightline associated with the intervening structures such as high velocity clouds (HVCs) in the Galactic halo and/or gas associated with the Local Group galaxies. The metal abundance of gas associated with the background galaxy can be determined from absorption spectra. This becomes particularly interesting when the background galaxy is a starburst galaxy: starburst galaxies release vast amounts of mass, energy, momentum and chemically-enriched gas into the surrounding intergalactic medium through supernova-driven galactic winds (e.g. Heckman et al., 1995). Deriving the metallicities of gas associated with outflows such as supershells, provides estimates of the chemical enrichment and star-formation history of the galaxy and an estimate of the extent starburst galaxies (especially dwarf galaxies) pollute the local intergalactic medium.

NGC 1705, a nearby (distance ~ 6 Mpc) H I-rich dwarf galaxy, contains the principal constituents of a starburst including a kpc-scale expanding shell (Meurer et al., 1992) and a luminous central superstar cluster, NGC 1705-1 (Sandage, 1978 & Melnick et al., 1995). The UV spectrum of NGC 1705-1 obtained using the Goddard High Resolution Spectrograph (*GHR*S) on the Hubble Space Telescope shows strong absorption lines which are interstellar in origin (Heckman & Leitherer, 1997). Using the same *GHR*S spectra, Sahu and Blades (1997; hereafter SB 97) reported the presence of three principal absorption systems at LSR velocities -20 km s^{-1} , 260 km s^{-1} and 540 km s^{-1} . They argued that the absorption features are interstellar rather than stellar in origin based on a comparison of the Si II $\lambda 1526.71 \text{ \AA}$ with the photospheric C III $\lambda 1175.7 \text{ \AA}$ absorption feature. The -20

km s^{-1} absorption line system was identified with Milky Way disk/halo gas and the 260 km s^{-1} system with an isolated high-velocity cloud HVC 487 associated with Magellanic Stream gas. The 540 km s^{-1} absorption system was identified with a blue-shifted emission component associated with a kpc-scale expanding supershell of ionized gas centered on NGC 1705-1. The most striking feature of the 540 km s^{-1} absorption line system is strong Si II and Al II absorption but weak Fe II $\lambda 1608 \text{ \AA}$ absorption. SB 97 interpreted the low intrinsic Fe abundance of the supershell component in the context of supernova-driven galactic wind evolution of dwarf galaxies.

In this paper, I extend the study of SB 97 to other atomic species and provide a list of interstellar absorption lines towards NGC 1705-1 in the $\lambda 1170$ to 1740 \AA range and their measured equivalent widths. Plots of the absorption in various atomic species together with the results of non-linear least square fit profiles are presented. Further arguments confirming the interstellar nature of the absorption features are outlined. The 540 km s^{-1} component associated with the supershell in NGC 1705 shows weak N I $\lambda 1200 \text{ \AA}$ triplet absorption which is further discussed in § 7.

2. The Observations and data reduction

The present study is based on two *GHRIS* spectra of NGC 1705-1 taken through the small science aperture with the G140L grating, which were retrieved from the HST Data Archives. The first spectrum extends from $\lambda 1170$ to 1462 \AA and the second one from $\lambda 1454$ to 1740 \AA . The velocity resolution of spectra are $\sim 140 \text{ km s}^{-1}$ at $\lambda 1200 \text{ \AA}$ and $\sim 100 \text{ km s}^{-1}$ at $\lambda 1700 \text{ \AA}$ and the signal-to-noise ratio (S/N) in the continuum ranges from $\sim 7:1$ at 1670 \AA to $16:1$ at 1400 \AA . These archival *GHRIS* spectra represent the highest S/N

and highest velocity resolution UV spectra ever taken towards NGC 1705-1. The reader is referred to SB 97 for details of the *GHRIS* data reduction procedures employed.

3. Presentation of the data

Between ~ 1300 and 1700 \AA , the continuum in the *GHRIS* spectra is smooth and slowly-varying (Figure 1 of Heckman & Leitherer 1997, shows the flux-calibrated *GHRIS* spectrum of NGC 1705-1). The spectra were normalized by fitting low-order polynomial functions and the continuum-normalized spectra between $\lambda 1175$ to 1740 \AA , are presented in Figures 1 (a – f). All absorption features with $> 3\sigma$ significance have been identified and the identifications are indicated in the figure with the following notation: \times indicates a photospheric absorption feature, \otimes indicates a blend and an unidentified line is indicated as ‘UL’. All features that have an interstellar origin (refer § 4) are entered in Table 2. Table 2 contains the equivalent measurements of the interstellar absorption lines at the -20 km s^{-1} , 260 km s^{-1} and 540 km s^{-1} (LSR velocities have been used throughout this paper). Equivalent width measurements of blended lines are uncertain and have not been listed in this table. The laboratory wavelengths and oscillator strengths are listed and the references are indicated in the footnote. The last part of the data presentation consists of plots of the interstellar absorption lines in the various atomic species together with the results of the non-linear least square profile fits (presented in § 5, 6 and 7).

E1

^{E1}NOTE TO EDITOR: Figure 1 (a – f)

4. Further evidence for interstellar origin of the absorption lines

Absorption features in the spectra of NGC 1705-1 can originate in (1) the interstellar medium of our Galaxy (2) in the intervening medium (3) in the interstellar medium of NGC 1705, or (4) in the stellar atmospheres of stars contributing to the UV flux of the galaxy. Previous studies of the interstellar absorption lines towards NGC 1705 have been made by York et al. (1990), using *IUE* spectra. They used both low-dispersion (velocity resolution $\sim 1000 \text{ km s}^{-1}$) as well as higher resolution *IUE* spectra (resolution $\sim 30 \text{ km s}^{-1}$) towards NGC 1705, to argue that the absorption lines seen in these spectra were primarily interstellar (also refer Heckman & Leitherer, 1997). SB 97 used the higher S/N *GHR*S data and confirmed the conclusions of York et al. (1990) that the UV absorption components seen in the NGC 1705 spectra are interstellar in origin.

The interstellar origin of the absorption lines is further supported in this paper by a compilation of all the photospheric lines present in the *GHR*S spectra (namely, C III $\lambda 1175 \text{ \AA}$, C III $\lambda 1247 \text{ \AA}$, Si III $\lambda 1294, 1296 \text{ \AA}$ and Si III $\lambda 1417 \text{ \AA}$). The photospheric profiles are shown in Figure 2 and the LSR recession velocity of NGC 1705 ($\sim 610 \text{ km s}^{-1}$) is indicated by an arrow. In all the cases, the photospheric absorption lines are weak, broad with FWHM ~ 200 to 300 km s^{-1} and have asymmetric blue-ward wings characteristic of stellar mass loss.

E2

The Si II $\lambda 1526.71 \text{ \AA}$ line has three narrow components : a strong feature centred at

^{E2}NOTE TO EDITOR: Figure 2

-20 km s^{-1} , a relatively weak feature centred at 260 km s^{-1} , and a strong feature centred at 540 km s^{-1} . All the other resonance lines in the spectra show similar velocity structure. Their velocities are not consistent with the systemic velocity of NGC 1705, nor do any of the profiles show asymmetric or P-Cygni shapes characteristic of stellar mass loss. Hence, apart from the broad, asymmetric C III 1175 Å, C III 1247 Å, Si III 1294, 1296 Å and Si III 1417 Å lines, the other lines can be attributed to an interstellar origin without ambiguity. The C IV and Si IV lines show features common to photospheric and interstellar lines: the three narrow components superposed on a broad asymmetric component (refer §5.3).

5. Interstellar absorption features

A simple curve-of-growth (cog) analysis for the three components at -20 km s^{-1} , 260 km s^{-1} and 540 km s^{-1} results in best-fitting b -values of $\sim 25 \text{ km s}^{-1}$, $\sim 50 \text{ km s}^{-1}$ and $\sim 30 \text{ km s}^{-1}$ respectively. The optical depths at the center of the line, τ_o , for the three absorption systems are listed in Table 1; only lines with $\tau_o \leq 1$ can be used for column density determinations ; stronger lines provide lower limits.

5.1. The neutral species

Narrow interstellar absorption lines of the N I λ 1200 Å triplet were detected in the spectra. The N I line is detected at -20 , 260 and 540 km s^{-1} . The N I λ 1200 Å triplet consists of three lines at 1199.6, 1200.2 and 1200.7 Å which have approximately the same strengths. The three lines of the N I triplet are blended on the *GHR*S spectra. In spite of this blending, it is apparent from Figure 3, that the absorption features at -20 and 260 km s^{-1} are moderately strong but conspicuously weak at 540 km s^{-1} (refer § 7). The

O I $\lambda 1302.2$ Å lines are detected but are heavily blended with the Si II $\lambda 1304.4$ Å line. Broad damped Lyman- α absorption is also detected (Figure 3). The damped Lyman- α absorption line gives a reasonably accurate measurement of the neutral hydrogen column densities, but because the absorption is strong there is very little information on the velocity components of the H I gas. The damped Lyman- α line was fitted with a theoretical Lyman- α damping profile. The fitting was initiated with two absorber velocities at -20 km s^{-1} and 540 km s^{-1} but the resulting profiles were unsatisfactory. The best fit was obtained for absorber velocities of 104 and 678 km s^{-1} and column densities $\log N = 20.1$ and 19.6 cm^{-2} respectively. The H I gas at ~ 678 km s^{-1} is probably H I gas associated with the dwarf galaxy. Information regarding the H I gas associated with the supershell at 540 km s^{-1} is impossible to disentangle.

E3

5.2. Singly-ionised species

Figure 4 is a plot of all the single ionized species detected in the *GHR*S spectra. Two resonance lines of singly ionized carbon, C II $\lambda 1334.53$ Å and C II* $\lambda 1335.71$ Å are detected. The velocity resolution is not sufficient, resulting in blending of these two lines. In addition there is a contribution from a broad, photospheric C II $\lambda 1334.53$ Å absorption feature, making it difficult to derive accurate equivalent widths.

Strong Al II $\lambda 1670.7$ Å absorption is present at both -20 and 540 km s^{-1} and has been

^{E3}NOTE TO EDITOR: Figure 3

extensively discussed in SB 97. The best observed species in the *GHRIS* spectra is Si^+ with five definite absorption line detections at $\lambda 1190.24$, 1193.29 , 1260.42 , 1304.37 and 1526.71\AA . For the -20 and 540 km s^{-1} components, with the exception of the $\lambda 1304.37 \text{\AA}$ line, all the other Si^+ lines have $\tau_{\circ} > 1$ and only lower limits to the column densities can be derived for these components. The 260 km s^{-1} component corresponding to HVC 487 has an optical depth of $\tau_{\circ} \leq 1$ at the centre of the line and has been used by SB 97 to derive a column density of $N(\text{Si}) = 4 \times 10^{13} \text{ cm}^{-2}$ and a metal abundance estimate $(\text{Si}/\text{H}) > 0.6(\text{Si}/\text{H})_{\odot}$ (see § 6)

$\text{S II } \lambda 1259.52 \text{\AA}$ absorption is present at the 3σ level at -20 and 540 km s^{-1} . Only one Fe II line at 1608.45\AA is covered by the *GHRIS* spectra. Strong Fe II absorption is detected at -20 km s^{-1} but only weak Fe II absorption is detected at 540 km s^{-1} . The low Fe/Al abundance ratio has been extensively discussed by SB 97. No $\text{Ni}^+ \lambda 1317.22\text{\AA}$ absorption is detected in the spectra at the 3σ level. ^{E4}

5.3. Higher ionization species

The $\text{Si III } \lambda 1206.50 \text{\AA}$ and the doublet resonance absorption lines of Si IV and C IV are detected and shown in Figure 5. The C IV and Si IV lines show features common photospheric and interstellar lines: the three narrow components superposed on a broad asymmetric component. The Si IV lines, in particular, are heavily contaminated by broad, asymmetric photospheric component. No attempt has been made to subtract this photospheric component. The C IV and Si IV observed profiles are shown in Figure 5,

^{E4}NOTE TO EDITOR: Figure 4

although no equivalent measurements have been made due to the large uncertainties caused by photospheric contamination.

E5

6. The high velocity cloud HVC 487

The NGC 1705-1 sight-line intercepts a region which is approximately 10° away from the outermost H I contours that envelops both the Large and Small Magellanic Clouds on 21-cm maps (Mathewson & Ford, 1984). The 260 km s^{-1} absorption component seen in the UV spectra is associated with the isolated high velocity cloud, HVC 487 on the 21-cm map, based on velocity agreement (SB 97). The location of HVC 487 with respect to the NGC 1705 sightline, the Magellanic Clouds and the Magellanic Stream is shown in Fig 6. The data presented in this figure is an unpublished H I map of this region obtained from the all-sky HVC survey of Wakker and van Woerden (1991). The (Si/H) obtained by SB 97 for HVC 487 is $0.9 (\text{Si}/\text{H})_\odot$, close to the metal abundance estimates for the Magellanic Stream (Lu et al. 1994). The velocity agreement together with the agreement in metal abundances, point to a Magellanic Stream origin for HVC 478.

E6

^{E5}NOTE TO EDITOR: Figure 5

^{E6}NOTE TO EDITOR: Figure 6

7. Low N abundance for the NGC 1705 supershell component?

Galactic halos (e.g. Bowen et al. 1996) and gas-rich dwarf galaxies (York et al. 1986) have been proposed as giving rise to QSO absorption line systems (QSOALS). Star-formation induced gas outflows like supershells, emanating from starburst galaxies are another viable cause of QSOALS because of the following reasons: (1) they produce line strengths, ionizations and velocity structures similar to gas-rich dwarf galaxies (2) supershells from starburst galaxies extend to several kpc away from the nucleus of the galaxy thereby increasing the galaxy absorption cross section and (3) shell-like structures are an ubiquitous component of the ISM of galaxies, for example, the H I supershells in the Milky Way (Heiles, 1990) and M 101 (Kamphuis et al. 1991). The supershell component in the NGC 1705 sightline is a possible low redshift analogue to QSOALS, making it an excellent sightline to study the age, chemical enrichment and star-formation history of a dwarf galaxy, namely, NGC 1705.

The N/Si and N/O abundance ratios are good indicators of the age and star-formation history of a galaxy. *Primary* nitrogen is produced in the AGB phase of the evolution of intermediate-mass stars (3 - 8 M_{\odot}) and the delayed release of *primary* N causes a galaxy to zig-zag on N/O versus O/H plots, as it evolves. This technique has been pioneered by Pagel and collaborators (e.g. Pagel et al., 1992): the position of a dwarf galaxy on a N/O versus O/H plot determines its star-formation history (refer Fig. 7, Garnett, 1990). If star-formation proceeds in bursts separated by quiescent periods, the N/O increases with time for a fixed O/H. For example, a dwarf galaxy with mass $10^8 M_{\odot}$ turns 1% of its mass into massive stars in a burst quickly increasing the oxygen abundance of the whole galaxy by a factor of 6 and moving on a 45° line to the lower right. Ejection of nitrogen from intermediate-mass stars then increases N/O at constant O/H after the starburst has faded

(Edmunds & Pagel, 1978, Renzini & Voli, 1981). A second burst of the same size again moves the galaxy to the lower right, but by a smaller amount.

This technique has been extended to damped Lyman- α galaxies by Pettini et al. (1995) who first reported that the $z_{abs} = 2.27936$ absorption system in the QSO 2348–147 sightline had significantly underabundant N indicative of *primary* N production. The O I interstellar lines are usually heavily saturated so the N/Si abundance ratio was used as a substitute for the N/O abundance ratio. Lu et al. (1998) extended this study to 15 damped Ly- α galaxies and interpreted the scatter in the N/Si versus Si/H plots as support for the delayed release of primary N production in intermediate-mass stars.

This same technique can be applied to the supershell component to determine the age and star-formation history of NGC 1705. Figure 7 shows a plot of relative intensities against LSR velocities in the N I 1200 Å line (shown as a solid histogram). Plotted over is the Si II 1526Å observed profile (as dashed histogram). The N I feature at 540 km s⁻¹ is much weaker than the corresponding Si II feature. In the diffuse ISM in our Galaxy, little or no N is accreted onto interstellar grains (Jenkins, 1987, Sofia et al. 1994), hence depletion onto dust cannot account for the weak N I absorption in the supershell component.

The age estimates for the superstar cluster NGC 1705-1 of 10 to 20 Myr, estimated by Heckman & Leitherer (1997), provide a natural explanation for the observed column densities and the underabundance of Fe (Type Ia SN product) and N (produced by intermediate stars) compared to Si and Al (produced by Type II SNe) implying the shell could have been formed by the first generation of stars ($< 10^8$ years) and is therefore not contaminated by products from either intermediate stars or Type Ia SNe (Wheeler et al.

1989). Although a nucleosynthetic enrichment interpretation for the low N abundance due to *primary* N production is consistent with the age of NGC 1705-1 and the various timescales, there are two important uncertainties: (1) Using the photoionization code *CLOUDY* (Ferland, 1993), a spectral type B3V for the ionizing source NGC 1705-1 (Melnick et al. 1985) and a plane-parallel cloud, the N I/N II is estimated to be ~ 2 , indicating a significant amount of nitrogen could be in higher ionization stages, and (2) the weak N I for the shell component could be the result of collisional ionization effects as suggested by Trapero et al. (1996).

The uncertainties in the total N abundance caused by photoionization and collisional ionization effects cannot be addressed by the *GHRIS* spectra discussed in this paper. Observations of the higher ionization stages of nitrogen like, N II λ 1084Å and N III λ 988Å (observable with *FUSE*) will allow an assessment of the effects of photoionization and collisional ionization. The main advantage of investigating N/Si abundance ratio in the supershell component over the damped Lyman- α galaxies is that there is no need to make assumptions regarding the ionization source or the absorber. The properties and age of the ionizing central star cluster NGC 1705-1 and the supershell are well-studied (e.g. Meurer et al. 1992) and the significance of collisional ionization effects can be assessed.

E7

^{E7}NOTE TO EDITOR: Figure 7

8. Summary

An analysis of *GHERS* spectra in the $\lambda 1170$ to 1462 \AA range towards NGC 1705-1, the superstar cluster in the nearby dwarf starburst galaxy, NGC 1705 at $\sim 120 \text{ km s}^{-1}$ is presented. These *GHERS* spectra represent the highest S/N and highest velocity resolution UV spectra ever taken towards NGC 1705-1. The main results of this analysis are:

- 1) The photospheric absorption lines C III $\lambda 1175 \text{ \AA}$, C III $\lambda 1247 \text{ \AA}$, Si III $\lambda 1294, 1296 \text{ \AA}$ and Si III $\lambda 1417 \text{ \AA}$ are weak, broad and asymmetric and distinctly different from the interstellar absorption lines. Interstellar absorption is detected in (i) neutral atoms (N I $\lambda 1200 \text{ \AA}$ triplet and O I $\lambda 1302 \text{ \AA}$) singly ionized atoms (Si II $\lambda 1190, 1193, 1260, 1304$ and 1526 \AA , S II $\lambda 1253 \text{ \AA}$, C II $\lambda 1334 \text{ \AA}$, C II* $\lambda 1336 \text{ \AA}$, Fe II $\lambda 1608 \text{ \AA}$ and Al II $\lambda 1670 \text{ \AA}$) and atoms in higher ionization states (Si III $\lambda 1206 \text{ \AA}$, Si IV $\lambda 1393, 1402 \text{ \AA}$ and C IV $\lambda 1548, 1550 \text{ \AA}$. The Si IV and C IV absorption features have both interstellar and photospheric contributions.
- 2) All absorption features with $> 3\sigma$ significance have been identified and equivalent measurements of the unblended lines are listed in Table 1. Plots of the interstellar absorption lines in the various atomic species together with the results of the non-linear least square profile fits are presented in Figs. 3, 4 and 5. Three interstellar absorption systems at LSR velocities of -20 km s^{-1} , 260 km s^{-1} and 540 km s^{-1} are detected : the -20 km s^{-1} absorption line system is associated with Milky Way disk/halo gas and the 260 km s^{-1} system with an isolated high-velocity cloud HVC 487 associated with Magellanic Stream gas. The 540 km s^{-1} absorption system is associated with a blue-shifted emission component of a kpc-scale expanding supershell of ionized gas centered on NGC 1705-1.
- 3) Large-scale H I 21-cm maps of the regions near the NGC 1705-1 sightline and Magellanic Stream region show the isolated high velocity cloud, HVC 487 (Fig. 6). Based on velocity and metallicity agreement, HVC 487 is probably associated with Magellanic Stream gas.
- 4) The 540 km s^{-1} absorption line system has strong Si II and Al II absorption but weak Fe II $\lambda 1608 \text{ \AA}$ absorption which Sahu & Blades (1997) interpreted in the context of

supernova-driven galactic wind evolution of dwarf galaxies. In this paper, the apparent low N abundance of this supershell component is reported. Although a nucleosynthetic enrichment interpretation for the low N abundance due to *primary* N production is consistent with the age of NGC 1705-1 of 10 to 20 Myr, deriving the N abundance using the N I $\lambda 1200$ Å triplet has uncertainties due to photoionization and collisional ionization effects. These uncertainties can only be addressed by future observations of the higher ionization lines N II $\lambda 1084$ Å and N III $\lambda 989$ Å.

I wish to thank Bart Wakker for providing the unpublished 21-cm data, Jim Lauroesch for discussions and an anonymous referee for helpful comments.

Table 1. Line list and equivalent width measurements of the interstellar absorption lines towards NGC 1705 in the λ 1170 to 1740 Å range

Species	λ_{vac} (Å)	f	EW (mÅ)			τ_{\circ}^a			Comments	Ref ^d
			-20 km s ⁻¹	260 km s ⁻¹	540 km s ⁻¹	-20	260	540		
Si II	1190.42	0.2502 ^b	449 ⁺²⁶ ₋₂₂	88 ⁺¹⁰ ₋₁₂	<i>blend</i>	3.9	0.25	...	blend Si II 1193	(1)
Si II	1193.29	0.4991 ^b	<i>blend</i>	101 ⁺²¹ ₋₂₃	636 ⁺³⁵ ₋₉₄	...	0.2	> 20	...	(2)
N I	1199.55	0.1328 ^b	330 ⁺⁴⁰ ₋₃₆	474 ⁺⁹³ ₋₂₇	166 ⁺³⁴ ₋₂₅	1.3	1.1	0.5	...	(2)
Si III	1206.50	1.669 ^b	698 ⁺³⁷ ₋₃₂	532 ⁺⁴⁵ ₋₅₂	1015 ⁺¹¹² ₋₇₀	>20	0.8	> 20	...	(2)
S II	1253.81	0.01088 ^b	151 ⁺⁶⁶ ₋₁₈	...	181 ⁺⁸⁶ ₋₅₆	0.4	...	0.26	...	(1)
Si II	1260.42	1.007 ^b	<i>blend</i>	<i>blend</i>	704 ⁺¹⁴ ₋₂₂	>20	...	(1)
O I	1302.17	0.0489 ^b	<i>blend</i>	<i>blend</i>	<i>blend</i>	(2)
Si II	1304.37	0.086 ^b	<i>blend</i>	157 ⁺⁴⁷ ₋₃₄	370 ⁺²⁷ ₋₁₉	...	0.42	1.85	...	(1)
C II	1334.53	0.01277 ^b	<i>blend</i>	<i>blend</i>	<i>blend</i>	(2)
C II*	1335.71	0.01149 ^b	<i>blend</i>	<i>blend</i>	<i>blend</i>	(2)
Si IV	1393.76	0.5140 ^b	<i>blend</i>	<i>blend</i>	<i>blend</i>	blend with photospheric Si IV	(2)
Si IV	1402.77	0.2553 ^b	<i>blend</i>	<i>blend</i>	<i>blend</i>	blend with photospheric Si IV	(2)
Si II	1526.71	0.110 ^c	399 ⁺³¹ ₋₃₀	239 ⁺⁶² ₋₂₈	661 ⁺²¹ ₋₁₉	5.5	0.4	8.6	...	(1)
C IV	1548.19	0.1908 ^b	<i>blend</i>	<i>blend</i>	<i>blend</i>	blend with photospheric C IV	(2)
C IV	1550.77	0.009522 ^b	<i>blend</i>	<i>blend</i>	<i>blend</i>	blend with photospheric C IV	(2)
Fe II	1608.45	0.062 ^b	314 ⁺⁶³ ₋₂₀	...	286 ⁺¹⁵ ₋₄₄	2.3	...	0.5	...	(1)
Al II	1670.79	1.88 ^b	508 ⁺⁷⁰ ₋₈₁	...	624 ⁺⁴⁵ ₋₂₀	6.4	...	11.4	...	(1)

^aoptical depth at the center of the line for the -20, 260 and 540 km s⁻¹ components

^bMorton, 1991

^cSpitzer & Fitzpatrick, 1993

^dReferences: (1) = SB 97 (2) = this work

REFERENCES

- Bowen, D. V., Blades, C. J. Pettini, M. 1996, ApJ, 464, 141
- Edmunds, M. G. & Pagel, B. E. J. 1978, MNRAS, 185, 77
- Ferland, G. J. 1993, University of Kentucky Center for Computational Science Internal Report
- Garnett, D. R. 1990, ApJ, 363, 142
- Heckman, T.M., Dahlem, M., Lehnert, M. D., Fabbiano, G., Gilmore, D. & Waller, W. H. 1995, ApJ, 448, 98
- Heckman, T. M. & Leitherer, C. 1997, AJ, 114, 69
- Jenkins, E. B. 1987, in Interstellar Processes, eds. D. J. Hollenbach & H. A. Thronson, Jr., D. Reidel Publishing Company, 533
- Heiles, C. 1990, ApJ, 354,483
- Kamphuis, J., Sancisi, R. & van der Hulst, T. 1991, A&A, 244, 253
- Lu, L., Savage, B. D. & Sembach, K. R. 1994, ApJ, 437, L119
- Lu, L., Sargent, W.L.W. & Barlow, T. A. 1998, AJ, 115, 55
- Mathewson, D. S. and Ford, V. L. 1984, Structure and Evolution of the Magellanic Clouds, eds. S. van den Bergh & K. S. de Boer, Dordrecht:Kluwer, 25
- Melnick, J., Moles, M. & Terlevich, R. 1985, A&A, 149, L24
- Meurer, G. R., Freeman, K. C., Dopita, M. A. and Cacciari, C. 1992, AJ, 103, 60

- Meurer, G. R., Heckman, T. M., Leitherer, C., Kinney, A. Robert, C. & Garnett, D. R.
1995, *AJ*, 110, 2665
- Morton, D. C. 1991, *ApJS*, 77, 119
- Pagel, B.E.J., Simonson, E. A., Terlevich, R. J. & Edmunds, M. G. 1992, *MNRAS*, 255, 325
- Pettini, M., Lipman, K. & Hunstead, R. W. 1995, *ApJ*, 451, 100
- Sahu, M. S. & Blades, J. C. 1997, *ApJ*, 484, L125
- Sandage, A. 1978, *AJ*, 83, 904
- Renzini, A. & Voli, M. 1981, *A&A*, 94, 175
- Sofia, U. J., Cardelli, J. A. & Savage, B. D. 1994, *ApJ*, 430, 650
- Spitzer, L., Jr. & Fitzpatrick, E. 1993, *ApJ*, 409, 299
- Wakker, B. P. & van Woerden, H. 1991, *A&A*, 250, 509
- Wheeler, J. C., Sneden, C. & Truran, J. W. 1989, *ARA&A*, 27, 279
- York, D. G., Dopita, M., Green, R. & Bechtold, J. 1986, *ApJ*, 291, 627
- York, D. G., Caulet, A., Rybski, P., Gallagher, J., Blades, J. C., Morton, D. C. &
Wamsteker, W. 1990, *ApJ*, 351, 412

Fig. 1.— (a–f). The continuum-normalized *GHR*S spectra towards NGC 1705 from $\lambda 1173$ to $\lambda 1740$ Å. All interstellar absorption features with $> 3\sigma$ significance are labelled in the figure : \times indicates an absorption feature with photospheric origin, \otimes indicates a blend and unidentified lines are indicated by UL. All absorption features with an interstellar origin (§ 4) are entered in Table 1.

Fig. 2.— The photospheric absorption features in the *GHR*S spectra are plotted against LSR velocity. Note the broad, asymmetric nature of the line profiles. The systemic velocity of ~ 610 km s $^{-1}$ derived from H I observations of NGC 1705, is shown by arrows. Compare the broad, photospheric absorption features with the three narrow interstellar absorption components seen in Figure 4 at -20 km s $^{-1}$, 260 km s $^{-1}$ and 540 km s $^{-1}$, shown with arrows on the Si II $\lambda 1526.71$ Å profile.

Fig. 3.— (a–c) Normalized interstellar absorption profiles in the neutral atomic species are plotted as histograms against LSR velocities. Results of the non-linear least square fits are plotted as continuous lines. The model fit for the N I profile includes contributions from the $\lambda 1199.55$, 1200.22 and 1200.71 Å lines of the N I triplet. The O I absorption features are blended with the Si II absorption features and no model-fitting was done due to confusion. The damped Lyman- α absorption line is shown in panel (c) together with the theoretical damped profile.

Fig. 4.— Normalized interstellar absorption profiles in the singly ionized atomic species are plotted as histograms against LSR velocities. Results of the non-linear least square fits are plotted as continuous lines. Note the strong absorption at 540 km s $^{-1}$ in the Si II, S II and Al II lines. The Fe II absorption at this velocity, on the hand, is relatively weak (Sahu & Blades, 1997)

Fig. 5.— Normalized interstellar absorption profiles in the higher ionization stages are

plotted as histograms against LSR velocities with the results of the non-linear least square fits plotted as continuous lines. The Si IV and C IV lines show three narrow interstellar features superposed on a broad, photospheric component. No profile fitting has been done for the Si IV and C IV lines because of the uncertainties caused by photospheric contamination.

Fig. 6.— Plot showing H I 21-cm distribution in the region near the NGC 1705 sightline in galactic coordinates. The contour levels are represent $N(\text{H I}) = 2 \times 10^{18}$, 5×10^{18} , 1×10^{19} , 5×10^{19} , 1×10^{20} and $5 \times 10^{20} \text{ cm}^{-2}$. The grey-scale represents the velocity field : white = 100 to 150 km s^{-1} , light grey = 150 to 200 km s^{-1} , medium grey = 200 to 250 km s^{-1} , dark grey = 250 to 300 km s^{-1} and black = 300 to 350 km s^{-1} . Si IV and C IV lines Based on velocity agreement, the 260 km s^{-1} absorption component seen on the *GHERS* spectra is associated with the small isolated high-velocity cloud HVC 487 (see §6). The metallicity obtained for this component and therefore HVC 487, is similar to the Magellanic Cloud and Magellanic Stream indicating close association.

Fig. 7.— Normalized interstellar absorption profiles of N I are plotted as solid histograms against LSR velocities. The Si II $\lambda 1526.71\text{\AA}$ profile is plotted over as a dotted histogram. Note the weak N I absorption at 540 km s^{-1} in comparison to the Si II absorption (see § 7).

NGC 1705

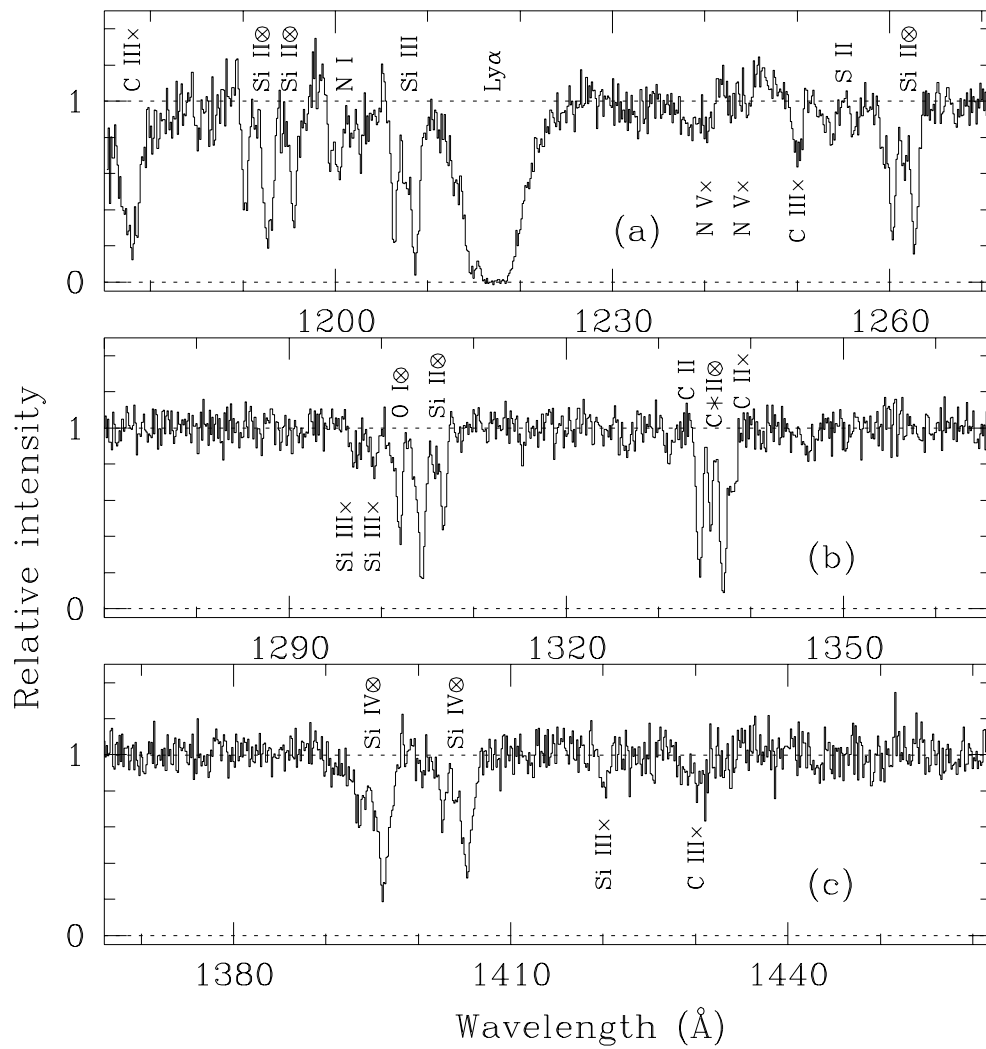


FIG. 1

NGC 1705

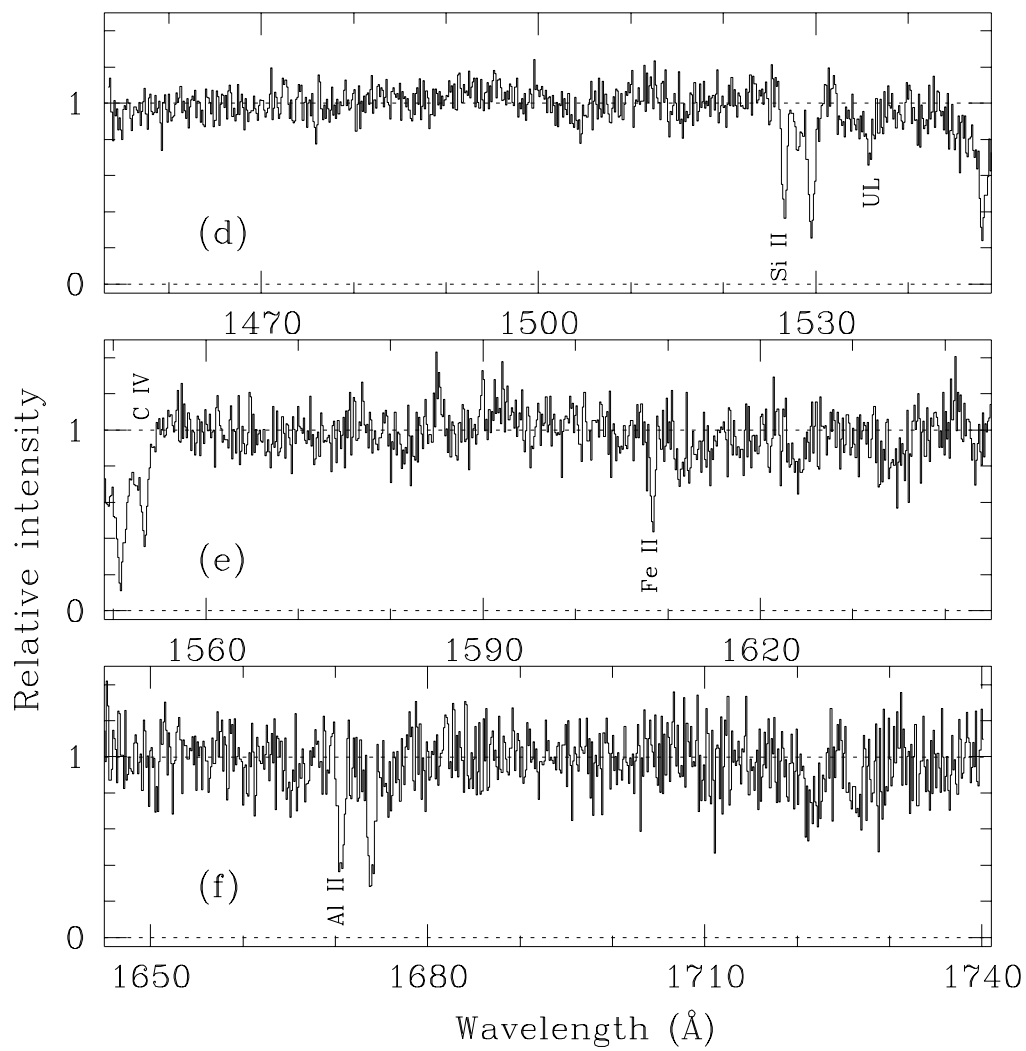


FIG.1

FIG. 2

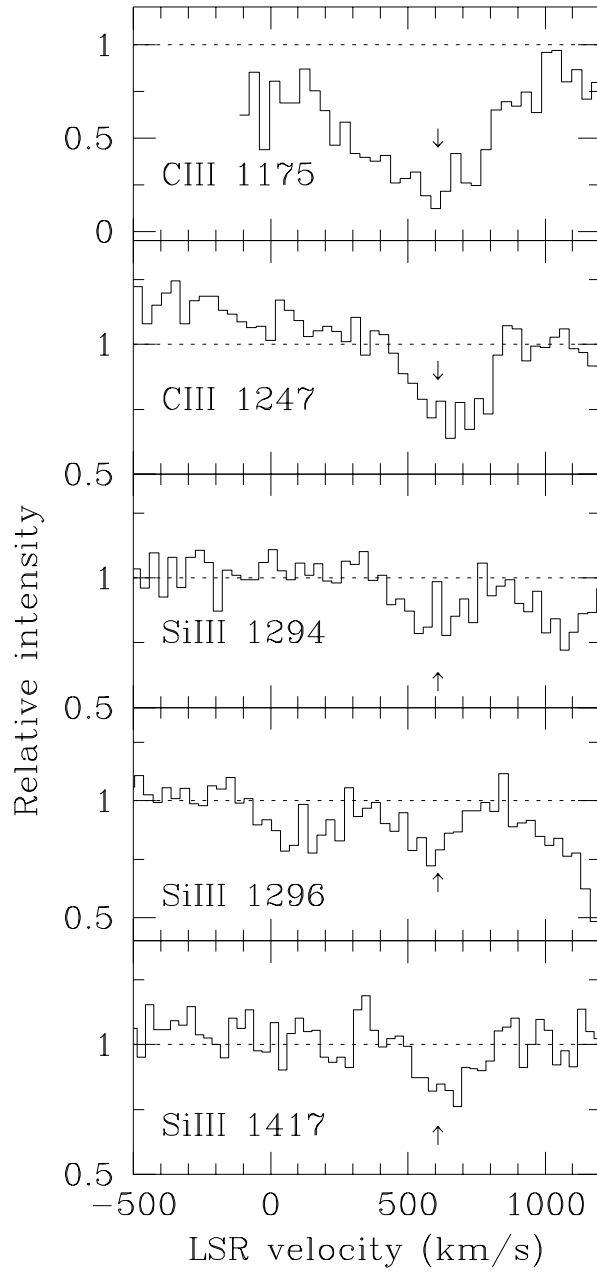


FIG. 3

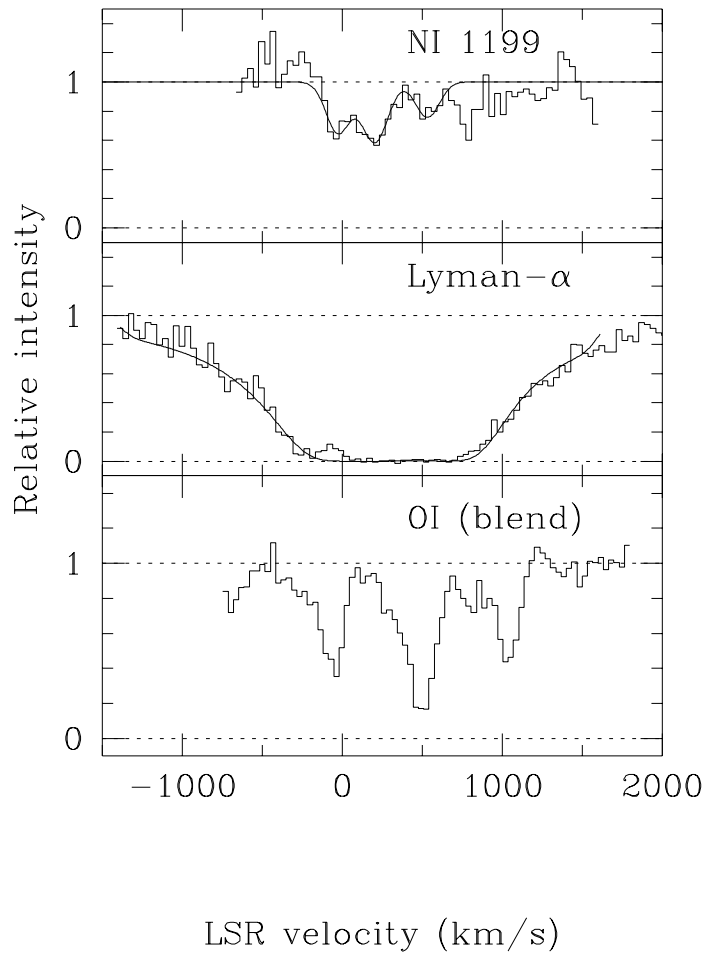


FIG. 4

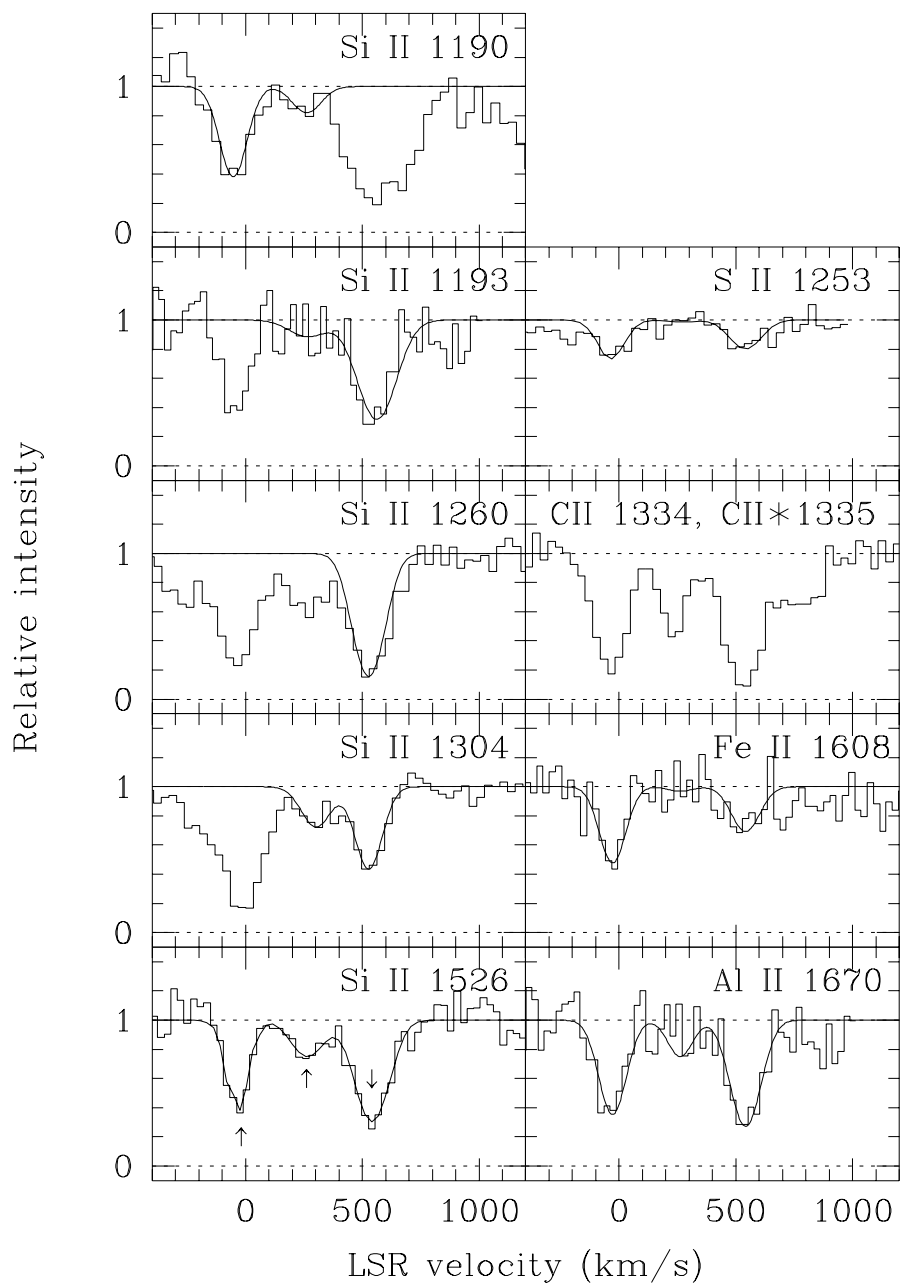
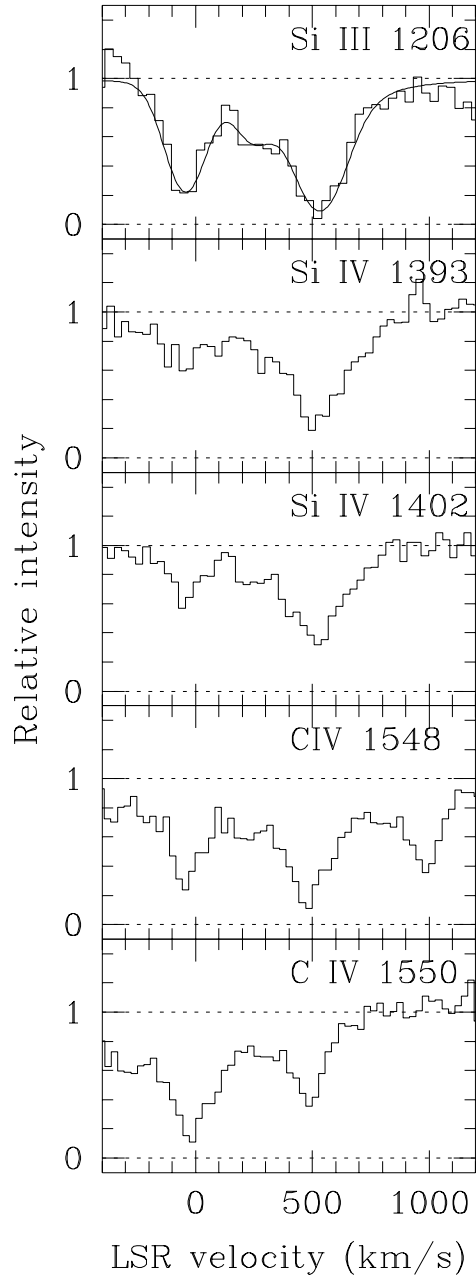


FIG. 5



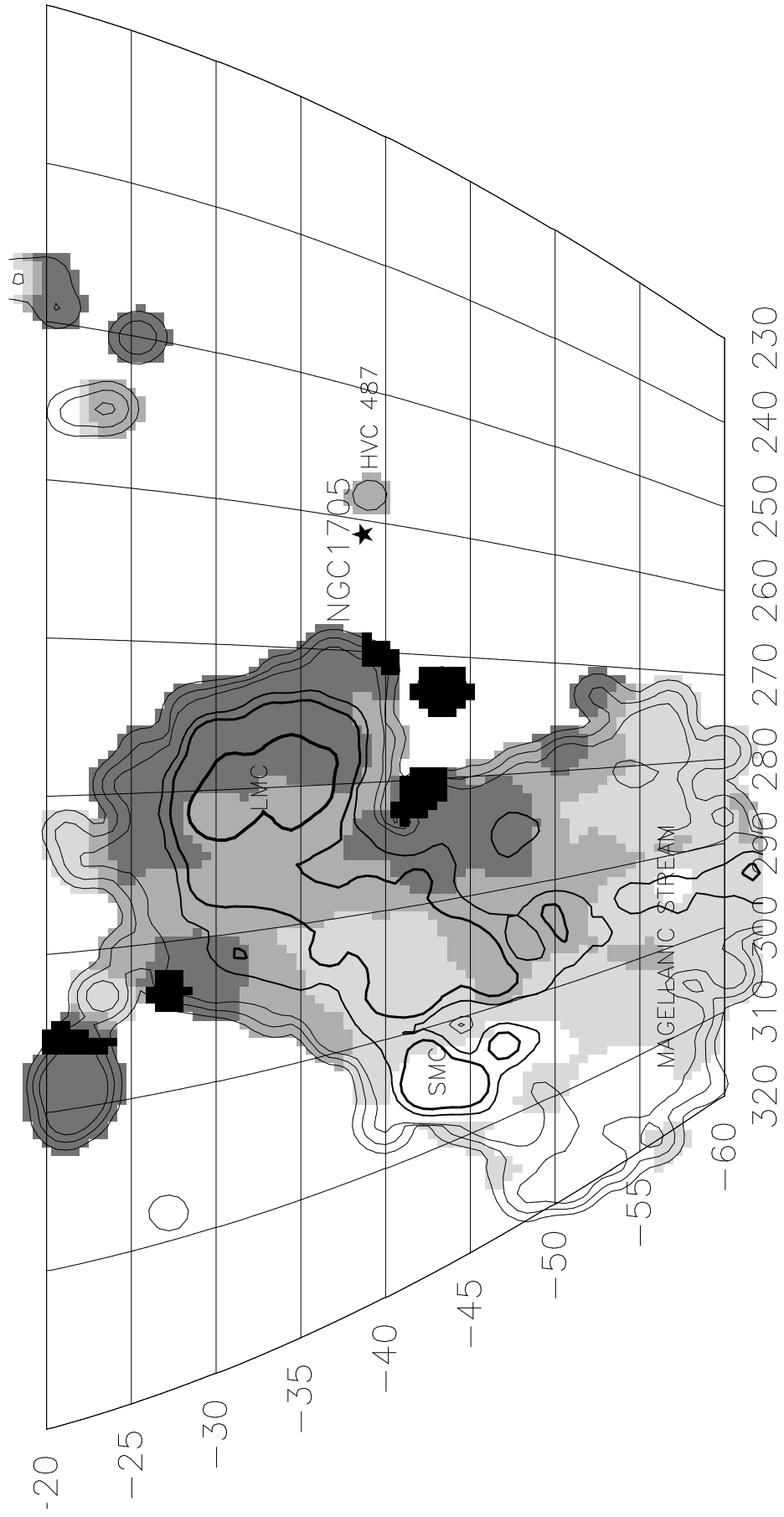


FIG. 7

